

Infrared Brazing of Ti₅₀Ni₅₀ Shape Memory Alloy and Inconel 600 Alloy with Two Ag-Cu-Ti Active Braze Alloys



REN-KAE SHIUE, SHYI-KAAN WU, and SHENG-HAO YANG

Infrared brazing of Ti₅₀Ni₅₀ SMA and Inconel 600 alloy using Cusil-ABA and Ticusil filler metals has been investigated. The joints were dominated by Ag-Cu eutectic with proeutectic Cu in the Cusil-ABA brazed joint and with proeutectic Ag in the Ticusil one. A continuous curved belt composed of a Ni₃Ti layer and a (Cu_xNi_{1-x})₂Ti layer formed in the brazed Ti₅₀Ni₅₀/Ticusil/Inconel 600 joint. On the Ti₅₀Ni₅₀ SMA side, an intermetallic layer of (Cu_xNi_{1-x})₂Ti formed in all joints, with *x* values around 0.81 and 0.47. Layers of (Cu_xNi_{1-x})₂Ti, Ni₃Ti, and mixed Ni₃Ti and Ni₂Cr intermetallics were observed next to the Inconel 600 substrate in the brazed Ti₅₀Ni₅₀/Cusil-ABA/Inconel 600 joint. The maximum shear strengths of the joints using the Cusil-ABA filler metal and the Ticusil filler metal were 324 and 300 MPa, respectively. In the Cusil-ABA brazed joint, cracks with cleavage-dominated fracture propagated along the (Cu_xNi_{1-x})₂Ti interfacial layer next to the Ti₅₀Ni₅₀ SMA substrate. In the Ticusil brazed joint, ductile dimple fracture occurred in the Ag-rich matrix near the Inconel 600 alloy substrate. The absence of a detrimental Ti-Fe-(Cu) layer on the Inconel 600 substrate side can effectively improve the shear strength of the joint.

DOI: 10.1007/s11661-016-3890-z

© The Minerals, Metals & Materials Society and ASM International 2016

I. INTRODUCTION

Ti₅₀Ni₅₀ shape memory alloy (SMA) undergoes a thermoelastic martensitic transformation and exhibits an excellent shape memory effect, superelasticity, and damping capacity.^[1,2] It has been applied in microelectro-mechanical systems such as micropumps and microactuators.^[3] In one application, shape memory actuators are used to replace exploding bolts utilized in petrochemical equipment and nuclear power plants.^[4] The shape memory actuator is joined with an infrastructure made of stainless steel or nickel-based alloy. Therefore, dissimilar brazing of Ti₅₀Ni₅₀ SMA and stainless steel/nickel-based alloy is an important issue in such an application.

In our previous study, dissimilar infrared brazing of Ti₅₀Ni₅₀ SMA and AISI 316L stainless steel (SS) using two silver-based active fillers, Cusil-ABA and Ticusil, was evaluated.^[5] The materials were successfully joined with maximal shear strengths of 237 MPa for Ticusil filler metal brazed at 1223 K (950 °C) for 60 seconds and only 66 MPa for Cusil-ABA filler metal brazed at 1143 K (870 °C) for 300 seconds. Experimental results indicated that the presence of the interfacial Ti-Fe-(Cu)

layer was detrimental to the shear strength of all joints. The 316L SS has a composition of Fe-17Cr-12Ni-2.5Mo (in wt pct),^[6] in which iron is the main element, and a Ti-Fe-(Cu) layer forms at the interface of the 316L SS side after infrared brazing. In order to prevent the formation of the brittle Ti-Fe-(Cu) layer, another Ni-based alloy, Inconel 600 alloy (Special Metals Corp., New Hartford, NY, USA) (Ni-14.0~17.0 Cr-6.0~10.0 Fe in wt pct), which has much less iron, was selected to study infrared brazing with Ti₅₀Ni₅₀ SMA.

Dissimilar brazing of Inconel 600 and ceramics has been reported previously.^[7-10] Chen et al. used traditional brazing to join Inconel 600 alloy to Si₃N₄ using Ag-27Cu-2Ti (in wt pct) filler metal and found that the bonding could be attributed to the diffusion of Ag and Cu along the grain boundaries of the Inconel 600 alloy.^[7] Lee brazed Inconel 600 alloy to Al₂O₃ using Ag-27Cu-3Ti (in wt pct) filler metal with a 150 μm thickness and found that, after brazing at 1113 K (840 °C) for 1200 seconds, the joints contained perimeter and zone cracks resulting in fracture.^[8] Inconel alloys are similar to 316L SS in that a stable and passivating oxide layer forms to protect the surface.^[11] Despite their excellent corrosive resistance, these oxide films also act as a barrier to the wettability between Inconel 600 and general Ag-Cu filler metals. Several studies have revealed that adding Ti to Ag-Cu brazing alloys can significantly improve the wettability while joining SS or ceramic oxides.^[12,13] Accordingly, Cusil-ABA (Ag-35.25Cu-1.75Ti in wt pct) and Ticusil (Ag-26.7Cu-4.5Ti in wt pct) filler metals were used in this study for brazing Ti₅₀Ni₅₀ SMA and Inconel 600 alloy.

REN-KAE SHIUE is with the Department of Materials Science and Engineering, National Taiwan University, Taipei 106, Taiwan, ROC. SHYI-KAAN WU is with the Department of Materials Science and Engineering, National Taiwan University, and also with the Department of Mechanical Engineering, National Taiwan University. Contact e-mail: skw@ntu.edu.tw SHENG-HAO YANG is with the Department of Mechanical Engineering, National Taiwan University.

Manuscript submitted February 26, 2016.

Article published online December 19, 2016

Infrared brazing is characterized by a fast heating rate of up to 50 K/s, which is much higher than that of most traditional furnace brazing.^[14] With accurate temperature control, it is highly suitable for evaluating the mechanism of early-stage reaction kinetics in brazing. In this study, infrared brazing was applied to join Ti₅₀Ni₅₀ SMA and Inconel 600 alloy using Cusil-ABA and Ticusil active silver-based filler metals. The wettability, interfacial reactions, microstructural evolution, and shear strengths of joints formed under various brazing conditions were systematically investigated.

II. EXPERIMENTAL PROCEDURE

A Ti₅₀Ni₅₀ ingot of about 120 g was prepared by a vacuum arc remelter from the raw materials of titanium (99.9 wt pct purity) and nickel (99.9 wt pct purity) and remelted six times in an argon atmosphere. The ingot was homogenized at 1173 K (900 °C) for 3600 seconds and then cut by a low-speed diamond saw to the specimen size. The specimens used in the experiment for wetting angle measurements and metallographical observations were templates with a size of 15 mm × 5 mm × 3 mm, and those used for shear tests were templates of 15 mm × 7 mm × 4 mm. The brazing surface was polished with SiC papers up to 1200 grit and subsequently cleaned using an ultrasonic bath with acetone as the fluid prior to brazing. Cusil-ABA and Ticusil brazing foils were purchased from Wesgo Company (The Morgan Crucible Company, Berkshire, England), and the thickness of these brazing foils was 50 μm. The chemical compositions and melting behaviors of these two brazing foils are listed in Table I.

The dynamic wetting angle of Cusil-ABA and Ticusil filler metals on Inconel 600 substrate was evaluated by sessile drop test using a filler ball of approximately 0.15 g in vacuum during the measurement. Schematic diagrams of the wetting angle measurement facility and the specimen holder during infrared brazing can be found in previous studies.^[14,15] An infrared heating furnace (ULVAC SINKU-RIKO RHL-P816C, Tokyo, Japan) was used as the main body of the vacuum furnace. A vacuum of 5×10^{-5} mbar was maintained, and the heating rate was set at 15 K/s throughout the experiment. Infrared rays were generated by infrared lamps, transmitted via a transparent quartz tube, and focused on the specimen holder. One end of the quartz tube was attached to the specimen holder, and the other end transmitted the signal into the image analysis system. The filler ball was located on the substrate,^[15] and a thermocouple was simultaneously in contact with the substrate. A graphite holder below the substrate was used to enhance the absorptivity of the infrared rays.

The heating conditions for dynamic wetting angle measurements used in the experiment were 1123 K and 1173 K (850 °C and 900 °C) for the Cusil-ABA filler metal, and 1173 K and 1223 K (900 °C and 950 °C) for the Ticusil filler metal, respectively, with holding times of 300 seconds for all heating conditions. The brazing conditions for metallographic observations and shear tests are summarized in Table II. All specimens, included those for dynamic wetting angle measurements, were preheated at 973 K (700 °C) for 300 s prior to brazing in order to equilibrate the temperature profile of the specimen.

Shear tests were performed to evaluate the bonding strength of the brazed joint, and the tests were carried out on three specimens for each brazing condition. A symmetrical double lap joint, Inconel 600/Ti₅₀Ni₅₀/Inconel 600, was used for shear testing of the brazed joint, as in previous studies.^[14,16] Figure 1 illustrates the schematic diagram of the shear test specimen enclosed in the graphite fixture, with the shaded areas in figure indicating infrared brazing. The two bold black lines, 3.5-mm wide, in the middle of the graph indicate the brazing filler metal. Shear tests were conducted using a Shimadzu AG-10 universal testing machine (Shimadzu Corp., Nakagyo-ku, Kyoto, Japan) with a constant crosshead speed of 0.0167 mm/s. Cross sections of infrared brazed joints were cut with a low-speed diamond saw and subsequently examined using a NOVA NANO 450 field emission gun scanning electron microscope (FESEM) (FEI Corp., Oregon, USA) equipped with an energy-dispersive spectrometer (EDS). Its operation voltage was 15 kV and the minimum spot size was 1 μm.

III. RESULTS AND DISCUSSION

A. Dynamic Wetting Angle Measurement

Figure 2 shows the results of dynamic wetting angle measurements of Cusil-ABA filler metal on Inconel 600 alloy at 1123 K and 1173 K (850 °C and 900 °C), and those of Ticusil filler metal on Inconel 600 alloy at 1173 K and 1223 K (900 °C and 950 °C), respectively. As shown in Figure 2, for Cusil-ABA filler metal, the wetting angles were 127 deg at 1123 K (850 °C) and 117 deg at 1173 K (900 °C) at the beginning. These angles remained almost constant in the first 30 or 40 seconds before continuously dropping to 65 deg (1123 K (850 °C) or 58 deg (1173 K (900 °C)) at 300 seconds. Also shown in Figure 2 are the results for Ticusil filler metal. At 1173 K (900 °C), the wetting angle also remained almost constant at 125 deg in the first 50 seconds before dropping dramatically to 95 deg

Table I. Chemical Compositions and Melting Temperatures of Two Brazing Foils

Braze Foil	Cusil-ABA	Ticusil
Chemical composition	63Ag-35.25Cu-1.75Ti (wt pct)	68.8Ag-26.7Cu-4.5Ti (wt pct)
Solidus temperature	1053 K (780 °C)	1103 K (830 °C)
Liquidus temperature	1088 K (815 °C)	1123 K (850 °C)

Table II. Summary of Infrared Brazing Conditions Used in the Experiment

Filler Foil	Brazing Temperature	Brazing Time
Cusil-ABA	1123 K (850 °C), 1173 K (900 °C)	300 s
Ticusil	1173K (900 °C), 1223 K (950 °C)	180 s

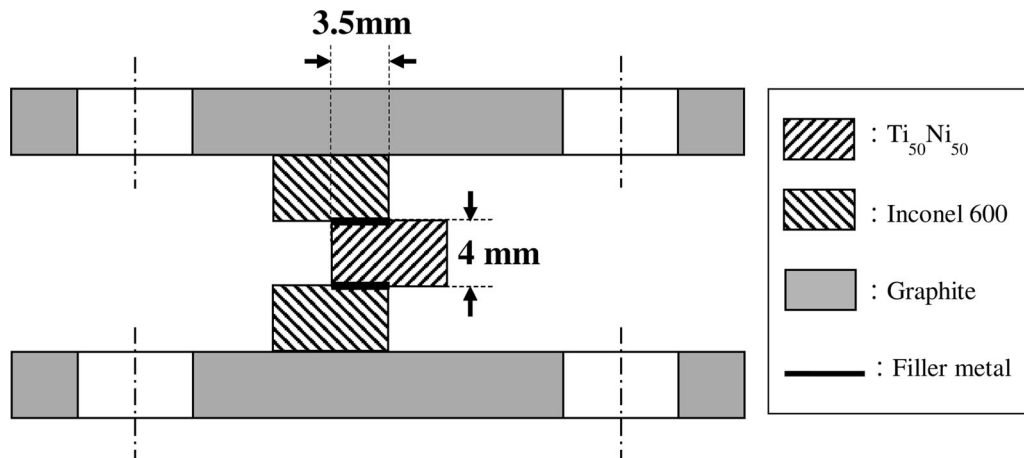


Fig. 1—Schematic diagram of the shear test specimen.^[14,16]

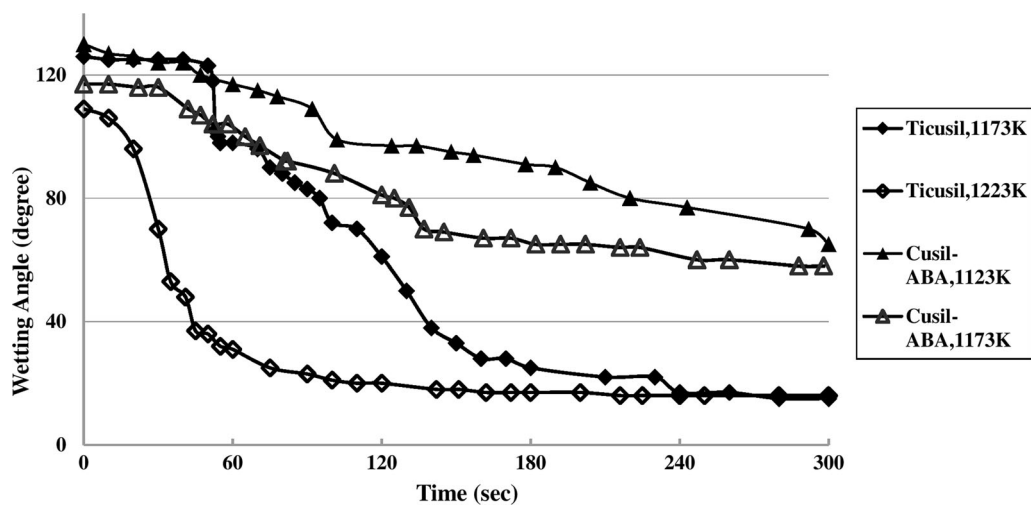
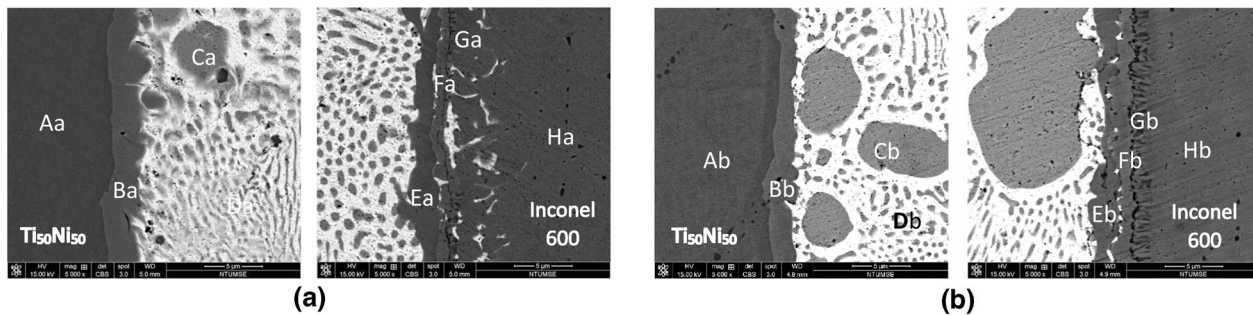


Fig. 2—Dynamic wetting angle measurements of Cusil-ABA and Ticusil filler metals on the Inconel 600 substrate.

at 50 seconds. It then decreased quickly to 25 deg at 160 seconds and continued to drop slowly to 18 deg at 300 seconds. At 1223 K (950 °C), the wetting angle dropped quickly in the first 50 seconds from 110 to 30 deg and then decreased slowly to 18 deg at 300 seconds. Capillarity and spreading are related to the balance of surface tensions, which determine the wetting and spreading behavior of a liquid on a solid, and interfacial reactions enhance the wetting of braze melt on the substrate.^[17–20] From Figure 2, one can find that, for Ticusil filler metal at 1223 K (950 °C), the braze melt reacted rapidly with the oxide layer(s) and then interacted with the substrate. However, the braze melt had almost no reaction with the oxide layers in the other heating conditions in the first 30 to 50 second at 1173 K

(900 °C). After that time, however, the melt began to react with the oxide layers and then with the substrate. The results of Figure 2 indicate that the Ticusil filler metal exhibited rather good wettability when the brazed specimen was tested at ≥ 1173 K (900 °C) for at least 180 seconds. However, the wettability of the Cusil-ABA filler metal was not as good as that of the Ticusil filler metal, and the wetting angles exceeded 50 deg for specimens tested at 1123 K and 1173 K (850 °C and 900 °C) for 300 seconds.

The results of dynamic wetting angle measurements for the balls of Cusil-ABA and Ticusil filler metals on $Ti_{50}Ni_{50}$ SMA at 1143 K and 1173 K (870 °C and 900 °C) have been reported previously.^[15] According to Reference 15 for all heating conditions, the wetting



at pct	Aa	Ab	Ba	Bb	Ca	Cb	Da	Db	Ea	Eb	Fa	Fb	Ga	Gb	Ha	Hb
Ti	49.8	50.1	31.2	34.4	-	4.1	-	-	30.1	31.6	27.0	26.6	18.5	12.3	-	-
Cu	-	-	35.7	31.1	92.4	92.8	48.1	44.3	36.5	33.6	6.1	6.3	-	-	-	-
Ni	50.2	49.9	33.1	34.5	2.9	-	-	-	33.4	34.8	66.0	64.0	50.9	48.6	73.7	73.6
Fe	-	-	-	-	-	-	-	-	-	-	-	3.1	10.3	8.5	9.2	9.1
Ag	-	-	-	-	4.7	3.1	51.9	55.7	-	-	0.9	-	-	-	-	-
Cr	-	-	-	-	-	-	-	-	-	-	-	-	20.3	30.6	17.1	17.3
Phase(s)	Ti ₅₀ Ni ₅₀	(Cu _x Ni _{1-x}) ₂ Ti	Cu-rich	Ag-Cu eutectic	(Cu _x Ni _{1-x}) ₂ Ti	Ni ₃ Ti	Ni ₃ Ti+Ni ₂ Cr	Inconel 600								

Fig. 3—SEM BEIs and EDS chemical analysis results of Ti₅₀Ni₅₀/Cusil-ABA/Inconel 600 infrared brazed at (a) 1123 K (850 °C) and (b) 1173 K (900 °C) for 300 s.

angle drops significantly in the first 20 seconds and then at 100 seconds reaches steady values of 30 and 15 deg for Cusil-ABA filler metal at 1143 K (870 °C) and 1173 K (900 °C), respectively, and values of 40 and 10 deg for Ticusil filler metal at 1143 K and 1173 K (870 °C and 900 °C), respectively. For both Cusil-ABA and Ticusil filler metals, their wettability with Ti₅₀Ni₅₀ SMA is much better than that with Inconel 600 alloy.

B. Microstructural Observations of Infrared Brazed Joints

1. Ti₅₀Ni₅₀/Cusil-ABA/Inconel 600 joints

The Ti₅₀Ni₅₀/Cusil-ABA/Inconel 600 joints infrared brazed at 1123 K and 1173 K (850 °C and 900 °C) for 300 seconds had cross-sectional widths of about 60 μm. Figures 3(a) and (b) shows the backscattered electron image (BEI) cross sections and EDS chemical analysis results of Ti₅₀Ni₅₀/Cusil-ABA/Inconel 600 specimens infrared brazed at 1123 K (850 °C) and 1173 K (900 °C) for 300 seconds, respectively. The infrared brazed joints were dominated by Ag-Cu eutectic (marked by Da and Db) and had interfacial layers on the Ti₅₀Ni₅₀ SMA side and on the Inconel 600 alloy side.

As shown in Figure 3, the area on the Ti₅₀Ni₅₀ substrate side primary consisted of a layer of (Cu_xNi_{1-x})₂Ti intermetallic (marked Ba and Bb) with different *x* values.^[21,22] The Ag penetrated along the grain boundaries of the (Cu_xNi_{1-x})₂Ti intermetallic layer. In addition, the Ag-Cu eutectic near the (Cu_xNi_{1-x})₂Ti layer had a few proeutectic Cu-rich areas (marked Ca and Cb). As shown in Figure 3, the area on the Inconel 600 substrate side formed three layers. Layer G (abbr. of Ga and Gb), neighboring the Inconel 600 substrate, had a lamellar structure, which was regarded as Ni₃Ti mixed with Ni₂Cr intermetallics. Layer F (abbr. of Fa and Fb), next to the lamellar structure G, was identified as Ni₃Ti alloyed with small amounts of Cu,

Fe, and Ag. Layer E (abbr. of Ea and Eb), located between layer F and the Ag-Cu eutectic, had a composition of Ti-30.1~31.6, Ni-33.4~34.8, and Cu-33.6~36.5 (in at pct), which was regarded as the (Cu_xNi_{1-x})₂Ti intermetallic. Similarly to layer B (abbr. of Ba and Bb), layer E also had Ag penetrating along the grain boundaries. Carefully examination of layers E revealed Ag agglomerations between layer E and layer F, which may have been Ag depleted from layers E and F during cooling.

C. Ti₅₀Ni₅₀/Ticusil/Inconel 600 Joints

Figure 4(a) shows the cross-sectional SEM BEI and EDS results of a Ti₅₀Ni₅₀/Ticusil/Inconel 600 joint infrared brazed at 1173 K (900 °C) for 180 seconds. The area on the Ti₅₀Ni₅₀ substrate side and that on the Inconel side are shown in Figures 4(b) and (c), respectively. The Ti₅₀Ni₅₀/Ticusil/Inconel 600 joint infrared brazed at 1173 K (900 °C) for 180 seconds had a cross-sectional width of about 45 μm, as shown in Figure 4(a). The width of Ti₅₀Ni₅₀/Ticusil/Inconel 600 joint was smaller than that of the Ti₅₀Ni₅₀/Cusil-ABA/Inconel 600 joint because more Ag-rich melt flowed out at the higher brazing temperature of the former.

The infrared brazed joint was dominated by the Ag-rich matrix and had a curved belt (layers C and D) in the middle of the brazed joint. On the left side of this curved belt, the braze was mainly composed of proeutectic Ag with a small area of Ag-Cu eutectic, but on the right side, the braze was almost all-proeutectic Ag-rich matrix, marked with E. This feature indicates that the consumption of Cu was much greater on the right side than that on the left side. As shown in Figures 4(b) and (c), two substrates, A and G, were Ti₅₀Ni₅₀ SMA and Inconel 600 alloy. Layers B and C were (Cu_xNi_{1-x})₂Ti intermetallics with different *x* values; layer D was identified as Ni₃Ti phase; and layer F was Ni₂Cr

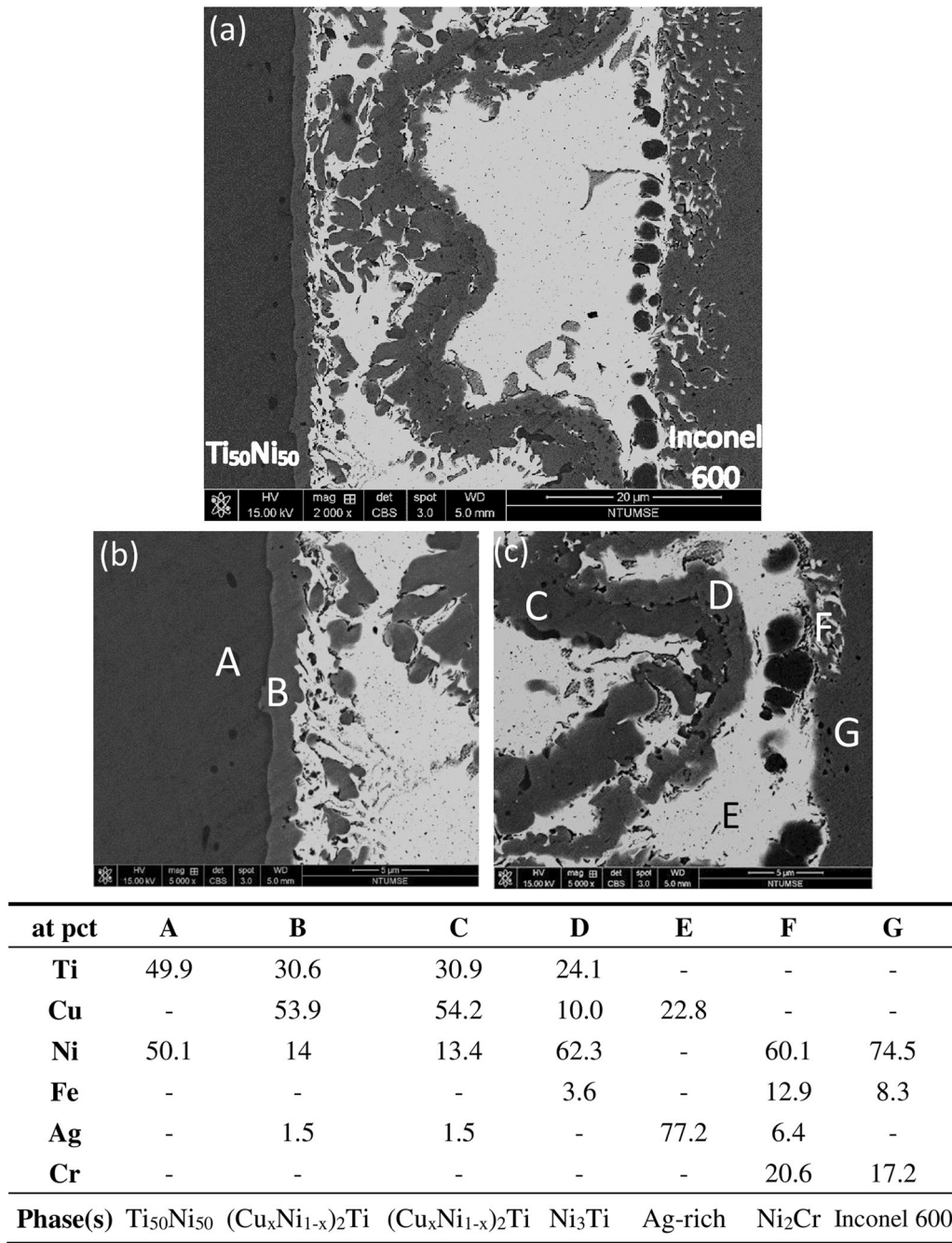
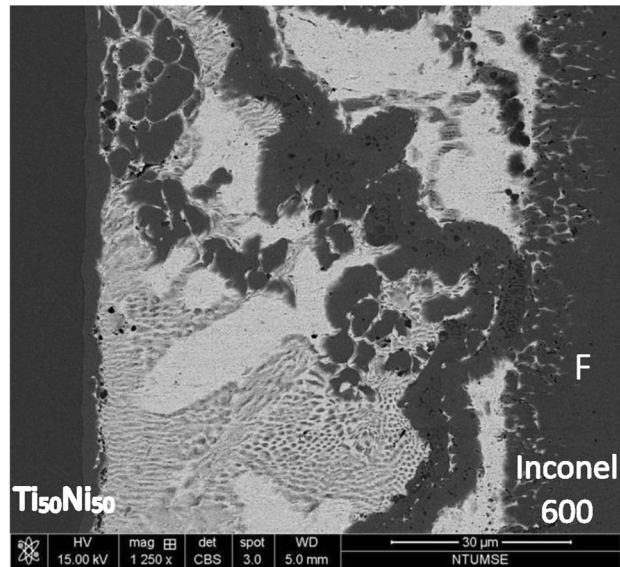


Fig. 4—SEM BEIs and EDS chemical analysis results of Ti₅₀Ni₅₀/Ticusil/Inconel 600 infrared brazed at 1173 K (900 °C) for 180 s: (a) cross section of the joint, (b) the Ti₅₀Ni₅₀ SMA substrate side, and (c) the Inconel 600 substrate side.

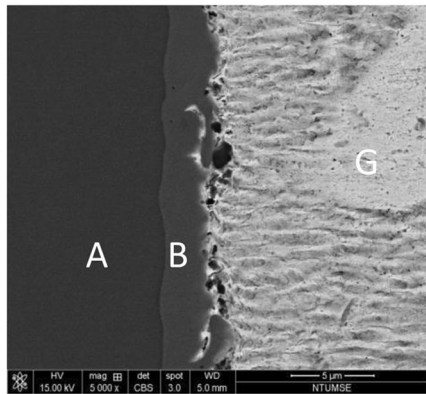
intermetallic with Ag existing along the grain boundaries. Layers C and D combined into a curved belt. At the same time, some small Ag agglomerations existed in the interface of layer C and layer D. However, the EDS chemical analysis results indicated that layer D contained much less Cu and much more Ni than layer C did. We suggest that the (Cu_xNi_{1-x})₂Ti intermetallic formed first causing the Cu content to decrease in the braze. At the same time, the dissolution of Ni atoms from the Inconel 600 substrate into the braze melt caused a Ni-rich Ni₃Ti phase of layer D to form in the

curved belt. The dissolution of Inconel 600 substrate into the braze melt was quite prominent.

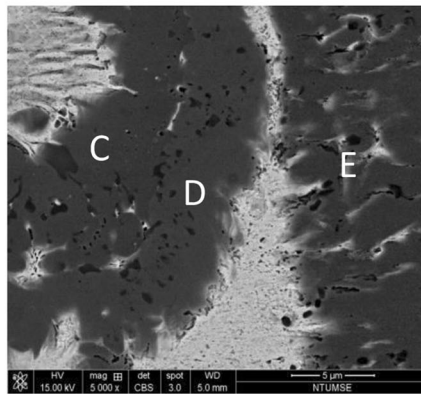
Figure 5(a) shows the cross-sectional SEM BEI and EDS results of a Ti₅₀Ni₅₀/Ticusil/Inconel 600 joint infrared brazed at 1223 K (950 °C) for 180 seconds. The area on the Ti₅₀Ni₅₀ substrate side and that on the Inconel 600 side are shown in Figures 5(b) and (c), respectively. As shown in Figure 5(a), the microstructure of the infrared brazed joint was dominated by the Ag-Cu eutectic and separated by a curved belt (marked layers C and D). The area on the left side of this curved



(a)



(b)



(c)

at pct	A	B	C	D	E	F	G
Ti	49.7	31.1	30.5	24.2	-	-	-
Cu	-	36.5	40.2	-	-	-	12.8
Ni	50.3	32.4	27.8	72.7	63.8	73.1	-
Fe	-	-	-	3.1	11.3	8.9	-
Ag	-	-	1.5	-	-	-	87.2
Cr	-	-	-	-	24.9	17.9	-
phase	Ti ₅₀ Ni ₅₀	(Cu _x Ni _{1-x}) ₂ Ti	(Cu _x Ni _{1-x}) ₂ Ti	Ni ₃ Ti	Ni ₂ Cr	Inconel 600	Ag-rich

Fig. 5—SEM BEIs and EDS chemical analysis results of Ti₅₀Ni₅₀/Ticusil/Inconel 600 infrared brazed at 1123 K (950 °C) for 180 s: (a) cross section of the joint, (b) the Ti₅₀Ni₅₀ SMA substrate side, and (c) the Inconel 600 substrate side.

belt was the Ag-Cu eutectic with minor proeutectic Ag, and that in the right side is mainly proeutectic Ag, indicating that most of Cu in the braze was depleted on the right side. As shown in Figures 5(b) and (c), the substrates A and F were Ti₅₀Ni₅₀ SMA and Inconel 600 alloy, respectively. Layers B and C were also (Cu_xNi_{1-x})₂Ti intermetallics with different *x* values, and layer D was identified as Ni₃Ti intermetallic. Layer E

was regarded as Ni₂Cr phase mixed with Ag existing at the grain boundaries.

D. Microstructural Evolution and the Related Reaction Mechanisms

Based on Figures 3, 4, and 5, the observed microstructural evolution and the related reaction

Table III. Average Shear Strengths of Infrared Brazed Joints

Filler Metal	Brazing Temperature	Brazing Time	Average Shear Strength
Cusil-ABA	1123 K (850 °C)	300 s	250 ± 17 MPa
	1173 K (900 °C)	300 s	324 ± 22 MPa
Ticusil	1173 K (900 °C)	180 s	288 ± 44 MPa
	1223 K (950 °C)	180 s	300 ± 10 MPa

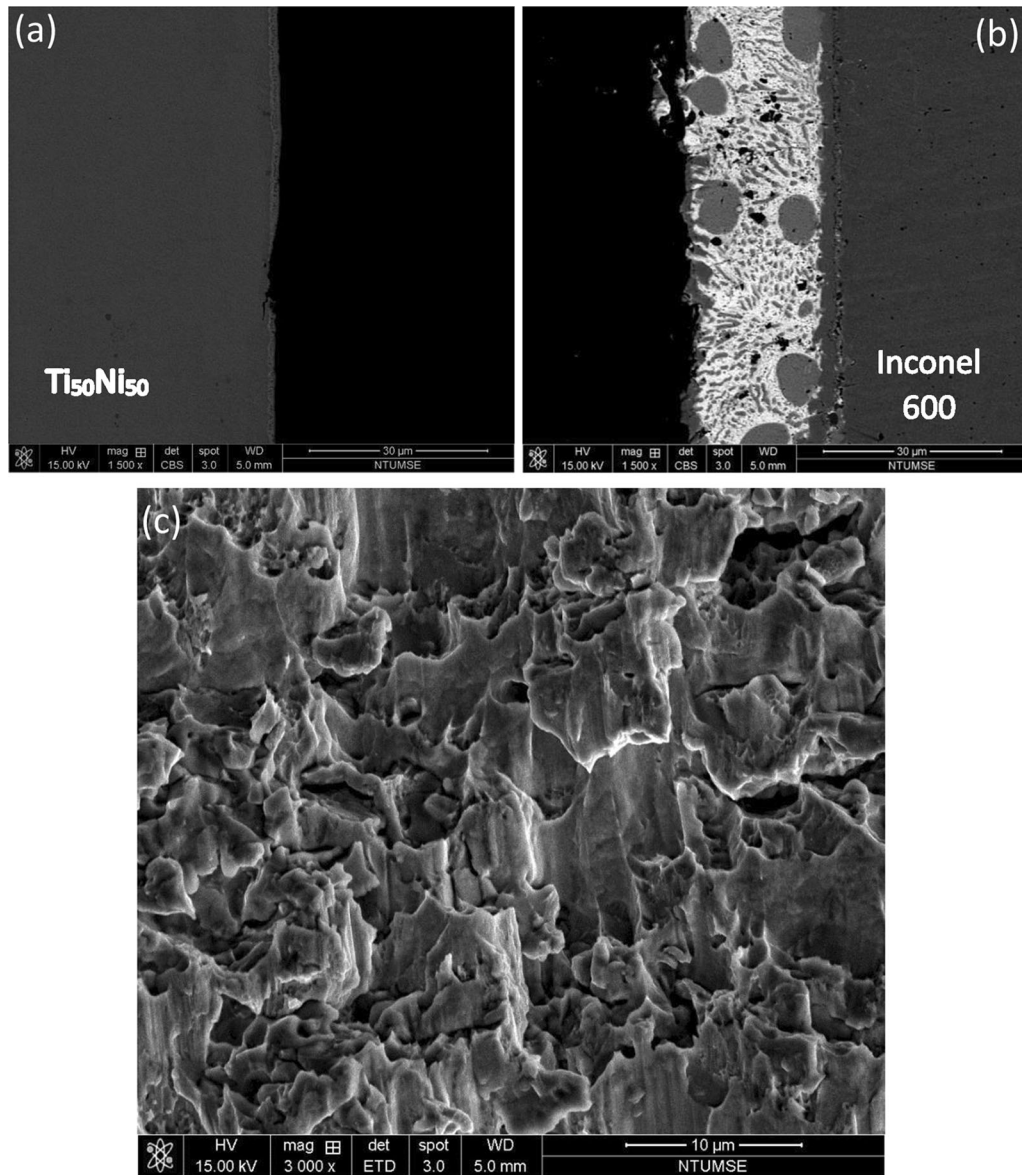


Fig. 6—SEM BEI cross sections of (a) Ti₅₀Ni₅₀ side, (b) Inconel 600 side, and (c) SEI fractograph of Ti₅₀Ni₅₀/Cusil-ABA/Inconel 600 joint infrared brazed at 1073 K (900 °C) for 300 s after shear test.

mechanisms on the two-substrate sides can be elucidated as follows. On the Ti₅₀Ni₅₀ substrate side, to identify the observed (Cu_xNi_{1-x})₂Ti intermetallics, the related phase diagram is important. According to the Cu-Ni-Ti ternary phase diagram, isothermally at 1143 K (870 °C), (Cu_xNi_{1-x})₂Ti intermetallic forms with x in the range of 0.20 to 0.82.^[21,22] (Cu_xNi_{1-x})₂Ti intermetallic compound was also reported at the interface of

the Ti₅₀Ni₅₀ SMA substrate and two other filler metals, pure Cu and Ti-15Cu-15Ni (in wt pct), infrared brazed at 1423 K and 1233 K (1150 °C and 960 °C), respectively.^[23] In Figure 4, the (Cu_xNi_{1-x})₂Ti intermetallic has an x value around 0.81. This value decreases to 0.58 shown in Figure 5, further to 0.54 at the Ba layer, and to 0.47 at the Bb layer shown in Figure 3. These results indicate that, for both the Cusil-ABA and the Ticusil

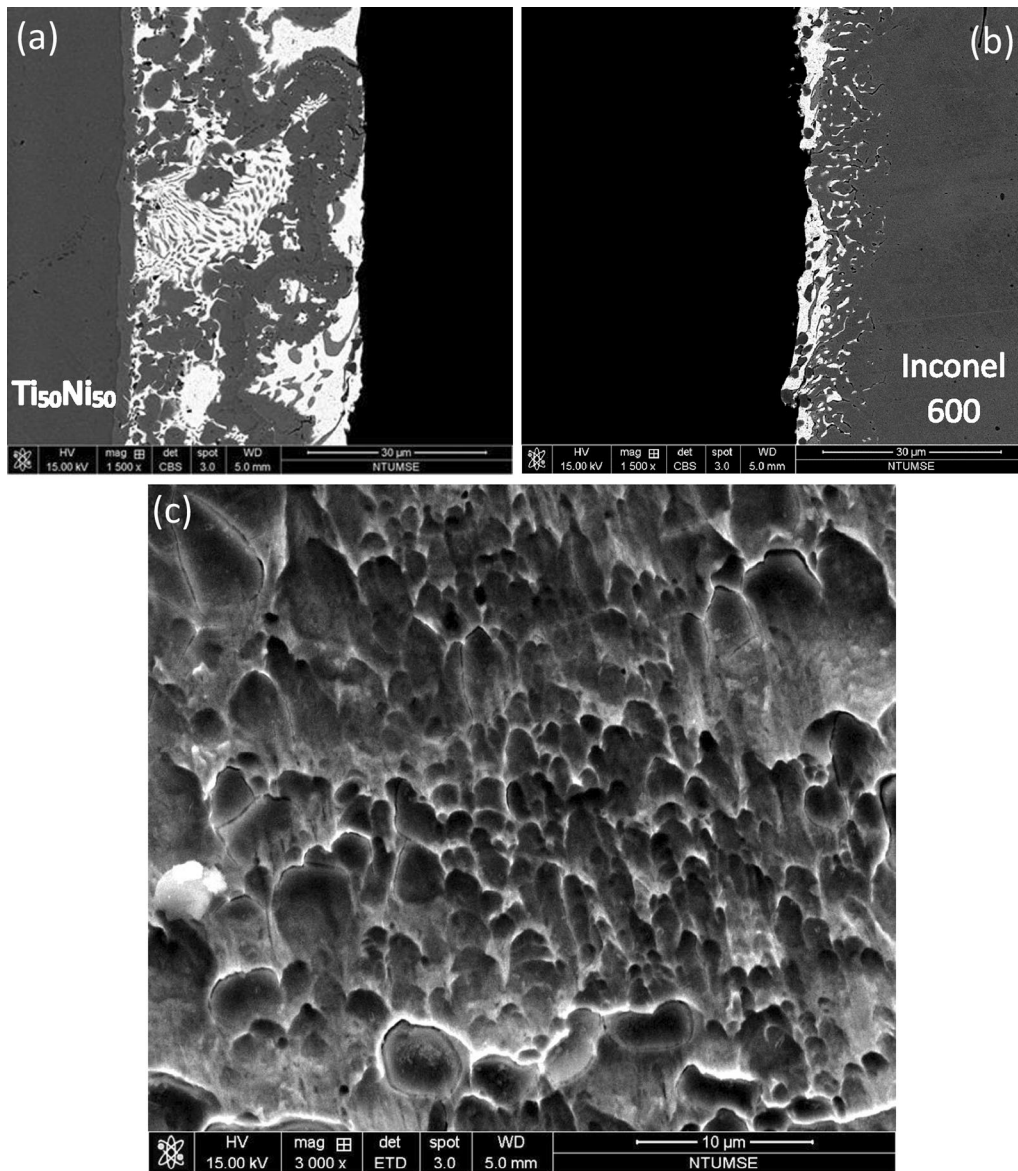


Fig. 7—SEM BEI cross sections of (a) $\text{Ti}_{50}\text{Ni}_{50}$ side, (b) Inconel 600 side, and (c) SEI fractograph of $\text{Ti}_{50}\text{Ni}_{50}$ /Ticusil/Inconel 600 joint infrared brazed at 1227 K (950 °C) for 180 s after shear test.

filler metals, the Cu content in $(\text{Cu}_x\text{Ni}_{1-x})_2\text{Ti}$ decreased as the brazing temperature increased, because more Ni atoms could dissolve from both substrates into the braze melt at higher brazing temperature. In addition, from comparing Figures 4(b) with 5(b), it appears that the smaller eutectic area along with the higher proeutectic Ag area in the braze of Figure 4(b) also meant that the amount of Cu was smaller in the braze matrix and the x value was higher in the $(\text{Cu}_x\text{Ni}_{1-x})_2\text{Ti}$ compound of Figure 4(b) than in that of Figure 5(b).

On the Inconel 600 substrate side, three major interfacial layers formed in the Cusil-ABA filler metal joints, as shown in Figure 3. The layers Ba/Bb and Ea/Eb were $(\text{Cu}_x\text{Ni}_{1-x})_2\text{Ti}$ intermetallics and were likely to have formed simultaneously. Because the formation of layers Ea and Eb needed the Inconel 600 substrate to supply Ni atoms, they formed as one of the interfacial

layers on the Inconel 600 substrate side. The layers Fa and Fb were identified as Ni_3Ti phase, which can conjugate with $(\text{Cu}_x\text{Ni}_{1-x})_2\text{Ti}$ intermetallic.^[21, 22] The layers Ga and Gb were lamellar and were thus regarded as mixtures of Ni_3Ti and Ni_2Cr intermetallics, for Ni_2Cr is the only intermetallic phase formed in the Ni-Cr binary phase diagram.^[24,25]

From Figures 3, 4, and 5, it appears that the interfacial layers formed on the Inconel 600 substrate side with Ticusil filler metal were quite different from those formed with Cusil-ABA filler metal. Layers E and F shown in Figure 3 were single layers neighboring the Inconel 600 substrate, but those shown in Figures 4 and 5 developed as a curved belt in the braze, separate from the Inconel 600 substrate. The formation of the curved belt in the braze can be ascribed to the fact that the Ticusil filler metal contains 4.5 wt pct Ti, and the Ni

atoms were supplied by dissolution of both substrates into the braze melt during brazing. In addition, the melting points of $(\text{Cu}_x\text{Ni}_{1-x})_2\text{Ti}$ and Ni_3Ti phases are higher than those of Ag-Cu eutectic and proeutectic, so the belt formed in a curved shape within the melt. Given the curved belt in the braze, the braze area shown in Figures 4(a) and 5(a) can be divided into two regions, the left region (from the belt to the $\text{Ti}_{50}\text{Ni}_{50}$ SMA substrate) and the right region (from the belt to the Inconel 600 substrate). Considering the EDS results shown in Figures 4 and 5, the $(\text{Cu}_x\text{Ni}_{1-x})_2\text{Ti}$ intermetallic shown in Figure 4 had higher Cu content than that shown in Figure 5. This means that the Cu content in the braze matrix of Figure 4 is lower than that in Figure 5, and therefore, the eutectic area in Figure 4 was smaller than that in Figure 5. In addition, the braze area in the right region had less Cu than that in the left region; this finding explains why the proeutectic Ag was mainly observed in the right region.

E. Microstructures and Shear Strengths of Infrared Brazed Joints

Table III shows the shear strengths of specimens formed under different brazing conditions. Increasing the brazing temperature increased the shear strength of the brazed joints with both fillers due to the better wettability of the fillers at higher brazing temperatures (Figure 2). The shear strengths of joints brazed at 1173 K (900 °C) for 300 seconds with Cusil-ABA filler metal and at 1223 K (950 °C) for 180 seconds with Ticusil filler metal were 324 and 300 MPa, respectively. Figure 6 presents SEM BEI cross sections and an SEI fractograph of the fractured $\text{Ti}_{50}\text{Ni}_{50}$ /Cusil-ABA/Inconel 600 joint brazed at 1173 K (900 °C) for 300 seconds. It can be seen clearly that the brazed specimen in Figures 6(a) and (b) fractured along the $(\text{Cu}_x\text{Ni}_{1-x})_2\text{Ti}$ intermetallic layer and the neighboring Ag-Cu eutectic. The fractograph shown in Figure 6(c) demonstrates cleavage-dominated fracture with little distortion. The EDS chemical analysis results are also consistent with those of layers Bb and areas Db in Figure 3(b).

Figure 7 shows SEM BEI cross sections and an SEI fractograph of the fractured $\text{Ti}_{50}\text{Ni}_{50}$ /Ticusil/Inconel 600 joint brazed at 1223 K (950 °C) for 180 seconds. According to Figures 7(a) and (b), the fracture was located on the right side of the curved belt and propagated along the Ag-rich matrix near the layer E of Figure 5. The ductile dimple fracture can be observed in Figure 7(c). Notably, the higher brazing temperature and Ti content of the Ticusil filler caused more vigorous reactions among Cu, Ni, and Ti. There was a large curved belt composed of $(\text{Cu}_x\text{Ni}_{1-x})_2\text{Ti}$ and Ni_3Ti layers in the middle of the brazed joint, as illustrated in Figures 4 and 5. Because the formation of this curved belt in the joint consumed Cu and Ti from the Ticusil filler metal, a Ag-rich dominated matrix developed. In contrast, the Ag-Cu eutectic dominated the Cusil-ABA brazed joint due to its lower Ti content and brazing temperature. It is obvious that the low yield strength of the Ag-rich matrix resulted in the dimple dominated fracture of the Ticusil brazed joint, as shown in Figure 7(c).

From Table III and Reference 5 it is clear that the shear strengths of $\text{Ti}_{50}\text{Ni}_{50}$ SMA and Inconel 600 joints are much higher than those of $\text{Ti}_{50}\text{Ni}_{50}$ SMA and AISI 316L SS when the same filler metal and the same infrared brazing conditions are used. For example, for Cusil-ABA filler metal brazed at 1173 K (900 °C) for 300 seconds, the shear strength of the latter joint was 54 MPa, but that of the former was 324 MPa; for Ticusil filler metal brazed at 1223 K (950 °C) for 180 seconds, the shear strength of the latter joint was 186 MPa, while that of the former was 300 MPa. These results clearly demonstrate that the detrimental Ti-Fe-(Cu) layer on the Inconel 600 substrate side decreases the shear strength of the joint; it follows that preventing the formation of that layer would increase the strength of the joint.

Intermetallic layer formation plays an important role in brazing $\text{Ti}_{50}\text{Ni}_{50}$ SMA and Ni/Fe-based alloys with Ag-based fillers. The dissolution of both substrates into the braze melt promotes vigorous reactions among Cu, Fe, Ni, and Ti during brazing. This study demonstrated that a Ti-Ni-(Cu) interfacial reaction layer is superior to a Ti-Fe-(Cu) one. As a result, the bonding strength of $\text{Ti}_{50}\text{Ni}_{50}$ SMA and Inconel 600 is higher than that of $\text{Ti}_{50}\text{Ni}_{50}$ SMA and 316L SS. It is deduced that the bonding strength of $\text{Ti}_{50}\text{Ni}_{50}$ SMA and Fe-based alloy can be improved if the reaction between Ti and Fe is retarded. For example, the application of Ni-clad 316L SS would be a good approach to ameliorate the joint strength between $\text{Ti}_{50}\text{Ni}_{50}$ SMA and 316L SS.

IV. CONCLUSIONS

The microstructural evolution and shear strength of $\text{Ti}_{50}\text{Ni}_{50}$ SMA and Inconel 600 alloy infrared brazed with Cusil-ABA and Ticusil filler metals at 1123 K and 1173 K (850 °C and 900 °C) for 300 seconds and at 1173 K (900 °C) and 1223 K (950 °C) for 180 seconds, respectively, are summarized below:

1. Measurements of the dynamic wetting angle indicate that Ticusil and Cusil-ABA filler metals, respectively, have excellent and good wettability on Inconel 600 alloy when the specimens are brazed at 1173 K and 1223 K (900 °C and 950 °C) for longer than 180 seconds with Ticusil filler metal and at 1123 K and 1173 K (850 °C and 900 °C) for at least 300 seconds with Cusil-ABA filler metal.
2. Infrared braze joints are dominated by the Ag-Cu eutectic with proeutectic Cu in Cusil-ABA joints and with proeutectic Ag in Ticusil joints. A continuous curved belt composed of a Ni_3Ti layer and a $(\text{Cu}_x\text{Ni}_{1-x})_2\text{Ti}$ layer forms in the brazed zone of brazed $\text{Ti}_{50}\text{Ni}_{50}$ /Ticusil/Inconel 600 joints and does not contact either of the two substrates.
3. On the $\text{Ti}_{50}\text{Ni}_{50}$ SMA side, a layer of $(\text{Cu}_x\text{Ni}_{1-x})_2\text{Ti}$ intermetallic forms in all joints with x values of around 0.81 and 0.58 for Ticusil filler metal brazed at 1173 K and 1223 K (900 °C and 950 °C) for 180 seconds, respectively, and of around 0.54 and 0.47 for Cusil-ABA filler metal brazed at 1123 K

and 1173 K (850 °C and 900 °C) for 300 seconds, respectively. This intermetallic results from the high Ni content in the braze melt due to enhanced dissolution of both substrates into the melt at higher brazing temperature or time.

4. On the Inconel 600 side, the Cusil-ABA joints are composed of a layer of $(\text{Cu}_x\text{Ni}_{1-x})_2\text{Ti}$ intermetallic, a layer of Ni_3Ti phase, and a layer of mixed Ni_3Ti and Ni_2Cr intermetallics next to the Inconel 600 substrate. The Ticusil joints have a layer of Ni_2Cr phase with Ag existing along the grain boundaries and neighboring the Inconel 600 substrate.
5. The maximum shear strengths of joints using Cusil-ABA filler metal and those using Ticusil filler metal are 324 and 300 MPa, respectively. In Cusil-ABA brazed joints, cracks with cleavage-dominated fracture propagate along the $(\text{Cu}_x\text{Ni}_{1-x})_2\text{Ti}$ intermetallic layer near the $\text{Ti}_{50}\text{Ni}_{50}$ SMA substrate. In Ticusil brazed joints, ductile dimple fracture of the Ag-rich matrix occurs near the Inconel 600 alloy substrate.

ACKNOWLEDGMENTS

The authors gratefully acknowledge the financial support for this research provided by the Ministry of Science and Technology (MOST) and National Taiwan University (NTU), Taiwan, under Grant Nos. MOST 104-2221-E002-005 and NTU 105R891803.

REFERENCES

1. K. Otsuka and C.M. Wayman: *Shape Memory Materials*, Cambridge University Press, London, 1998.

2. K. Otsuka and X. Ren: *Prog. Mater. Sci.*, 2005, vol. 50, pp. 511–678.
3. K. Krulevitch, A.P. Lee, P.B. Ramsey, J.C. Trevino, J. Hamilton, and M.A. Northrup: *J. Microelectron. Syst.*, 1996, vol. 5, p. 270.
4. L.McD. Schetky: *Trans. Mater. Res. Soc. Jpn.*, 1994, vol. 18B, pp. 1131–42.
5. R.K. Shiue, C.P. Chen, and S.K. Wu: *Metall. Mater. Trans. A*, 2015, vol. 46A, pp. 2364–71.
6. W.F. Smith: *Structure and Properties of Engineering Alloys*, 2nd ed., McGraw-Hill Co. Ltd., New York, 1993, pp. 494–98.
7. J.H. Chen, G.Z. Wang, K. Nogi, M. Kamai, N. Sato, and N. Iwamoto: *J. Mater. Sci.*, 1993, vol. 28, pp. 2933–42.
8. W.C. Lee: *J. Mater. Sci. Lett.*, 1996, vol. 15, pp. 29–31.
9. T. Zaharinie, F. Yusof, M. Fadzil, M. Hamdi, and T. Ariga: *Mater. Res. Innov.*, 2014, vol. 18 (S6), pp. 68–72.
10. A. Laik, P. Mishra, K. Bhanumurthy, G.B. Kale, and B.P. Kashyap: *Acta Mater.*, 2013, vol. 61, pp. 126–38.
11. M.F. Montemor, M.G.S. Ferreira, N.E. Hakiki, and M. Da Cunha Belo: *Corr. Sci.*, 2000, vol. 42, pp. 1635–50.
12. A.P. Xian and Z.Y. Si: *J. Mater. Sci.*, 1993, vol. 25, pp. 4483–87.
13. X. Yue, P. He, J.C. Feng, J.H. Zhang, and F.Q. Zhu: *Mater. Charact.*, 2008, vol. 59, pp. 1721–27.
14. R.K. Shiue, S.K. Wu, and S.Y. Chen: *Acta Mater.*, 2003, vol. 51, pp. 1991–2004.
15. R.H. Shiue and S.K. Wu: *Intermetallics*, 2006, vol. 14, pp. 630–638.
16. R.K. Shiue, Y.H. Chen, and S.K. Wu: *Metall. Mater. Trans. A*, 2013, vol. 44A, pp. 4454–60.
17. M. Schwartz: *Brazing: for the Engineering Technologist*, Chapman & Hall, New York, 1995, pp. 109–111.
18. P. Siegmund, C. Guhl, E. Schmidt, A. Rossberg, and M. Rettenmayr: *J. Mater. Sci.*, 2016, vol. 51, pp. 3693–3700.
19. A. Laik, A.A. Shirzadi, R. Tewari, A. Kumar, T. Jayakumar, and G.K. Dey: *Metall. Mater. Trans. A*, 2013, vol. 44A, pp. 2212–25.
20. Y. Liu, Z.R. Huang, and X.J. Liu: *Ceram. Int.*, 2009, vol. 35, pp. 3479–84.
21. P. Villars, A. Prince, and H. Okamoto: *Handbook of Ternary Alloy Phase Diagrams*, ASM International, Materials Park, 1995.
22. K.P. Gupta: *Phase Diagrams of Ternary Nickel Alloys*, Indian Institute of Metals, Calcutta, 1990.
23. T.Y. Yang, R.K. Shiue, and S.K. Wu: *Intermetallics*, 2004, vol. 12, pp. 1285–1292.
24. ASM Materials Handbook: *Binary Phase Diagrams*, ASM International, Materials Park, 1992, vol. 3, 9.2.155.
25. T.B. Massalski: *Binary Alloy Phase Diagrams*, ASM International, Materials Park, 1992.